Analysis of an N-Way Radial Cavity Divider with a Coaxial Central Port and Waveguide Output Ports

Marek E. Bialkowski, *Senior Member, IEEE*, and Vesa P. Waris, *Student Member, IEEE*

***Abstract*— A field matching technique is used to analyze an N-way divider which includes a radial cavity with a coaxial central port and H-plane coupled rectangular waveguide output ports. Dielectric coated and disc ended probes at the central port are considered. The analysis is divided into two parts. Part one is associated with the modeling of the central port and part two is concerned with the modeling of the waveguide peripheral ports. The analysis is simplified by assuming that the interaction between the central port and the peripheral ports is by means of axially symmetric radial waves which are uniform with cavity's height. Based on this analysis, algorithms are developed for calculating the scattering parameters of this structure using a PC. These algorithms show good agreement when tested against a finite element package (HFSS) and against measurements.**

I. Introduction

IN ORDER to increase the output power from microwave solid-state devices, power combining techniques can be used. Typically this includes three stages: dividing a signal to a number of individual amplifiers; amplification by each of the individual amplifiers; and combining each of the amplified signals. To achieve the function of signal division and combination, microwave structures known as divider/combiners can be employed. Many different divider/combiners have been proposed and investigated in the literature [1]–[8], using various microwave transmission media. Often waveguide technology is superior for many applications due to its low loss and high power handling, its relatively large operational bandwidth, and its compactness. Additionally, waveguide type divider/combiners have the potential to combine a large number of amplifiers.

A particular class of waveguide dividers arises from the parallel-plate (radial waveguide) structure. Radial waveguide divider/combiners with coaxial or conical probes have been thoroughly investigated [6]–[8], and computer algorithms and design strategies for their analysis have been developed. In applications where high power levels are of a particular concern, divider/combiners with waveguide ports are often preferred. This is for reasons of compatibility with solid-state amplifiers which usually incorporate waveguide ports, as well as for their increased power handling capabilities.

Manuscript received July 26, 1995; revised July 22, 1996. This work was supported in part by the Australian Research Council, Hewlett Packard, and MITEC, Ltd., Australia.

The authors are with the Department of Electrical and Computer Engineering, The University of Queensland, Queensland 4072, Australia.

Publisher Item Identifier S 0018-9480(96)07916-1.

In this paper, a radial waveguide divider/combiner with a coaxial central port and rectangular waveguide output ports is analyzed using a field matching method (FMM). Approximations concerning the interaction of the central port and the peripheral ports are introduced. These approximations make the analysis less involved while still preserving high computational accuracy. Based on this analysis, computer software was developed for a PC, providing a full set of scattering parameters at a single frequency point in a matter of seconds.

II. Analysis

Fig. 1 shows the configuration of the analyzed $N+1$ port structure. It consists of a radial cavity of radius R_b and height B, a central port (#0) in the form of a coaxial probe positioned inside the cylindrical region $0 < r < R_a$, and N identical rectangular waveguide peripheral ports of width A and height B. Although in a typical divider, the output ports are evenly spread along the guide's periphery, here, for the sake of generality, the waveguides are assumed to be arbitrarily positioned at angles θ_i, $i = 1, 2, \cdots, N$. The subtended angle of an individual rectangular guide as observed from the cavity's center is given by θ_w. Two types of coaxial probes, as shown in Fig. 1(b) and (c), are considered. This is due to the availability of the software for the analysis of these probe types in an infinite radial guide [9]–[11].

In order to simplify the analysis, the following assumptions are made.

1) The frequency of operation of the device is such that the rectangular waveguides support only the dominant TE_{10} mode. The higher order TE_{n0} rectangular waveguide modes, being constant with waveguide height but varying with width, are excited at the junctions between the rectangular waveguides and the cavity but rapidly decay with distance from the junction.
2) The radial cavity supports the propagation of radial waves which are uniform with height (y). Higher order radial waves which vary with height are excited by the central probe but they also decay with distance. Assuming that the distance between the central probe and the side wall of the cavity is large enough, the interaction between the coaxial probe and the peripheral ports by means of these higher order modes may be neglected. This is equivalent to the assumption that the higher order radial waves (varying with height) which are launched by the probe see a match terminated radial guide.

3) The diameter of the central probe is small in comparison with a free space wavelength so that the interaction between the probe and the peripheral ports is predominantly due to the radial waves which are axially symmetric with respect to the central probe. The interaction via azimuthally varying radial waves is neglected. This is equivalent to the assumption that the azimuthally varying waves which are launched from the peripheral ports do not see the probe.
4) Due to the form of excitation, the cavity supports TM to y radial waveguide modes [14].
5) The coaxial line only supports the propagation of its dominant TEM mode.

Due to the above assumptions, the task of modeling the entire divider/combiner's structure can be divided into two separate problems of a) modeling the coaxial probe and b) modeling the peripheral ports.

The solutions to these two problems are given in the following sections.

A. Central Probe Modeling

The disc-ended and dielectric coated coaxial probes radiating into an infinite radial guide have already been thoroughly investigated in the microwave literature [8]–[12]. However, the models developed in [9]–[12] cater only for determining the input impedance at the coaxial central port. For the current application, the coaxial probe has to be viewed as a two-port network with port #0 being a coaxial entry and port #R being a circular surface at $r = R_b$.

For the purposes of further analysis, port #0 is characterized in terms of an ordinary impedance (1)

1) When the interaction between the waveguide ports and the central post is described in an exact manner: $G_p = 1$ for all values of p.
2) When the interaction between the waveguide ports and the central post is approximated, so that $G_0 = 1$, and $G_p = 0$ for $p \neq 0$.

$$Z_0 = \frac{V}{I} \tag{1}$$

where V and I represent the voltage and current respectively at the coaxial entry.

Unlike port #0, port #R is characterized in terms of the radial wave impedance as observed by axially symmetric waves in the radial cavity. This impedance is defined by (2)

$$Z_R = \frac{\int_0^{2\pi} E_y(r = R_b)\, d\phi}{\int_0^{2\pi} H_\phi(r = R_b)\, d\phi} \tag{2}$$

where $E_y(r = R_b)$ is the y-component of the electric field and $H_\phi(r = R_b)$ is the ϕ-component of the magnetic field at the cylindrical surface $r = R_b$.

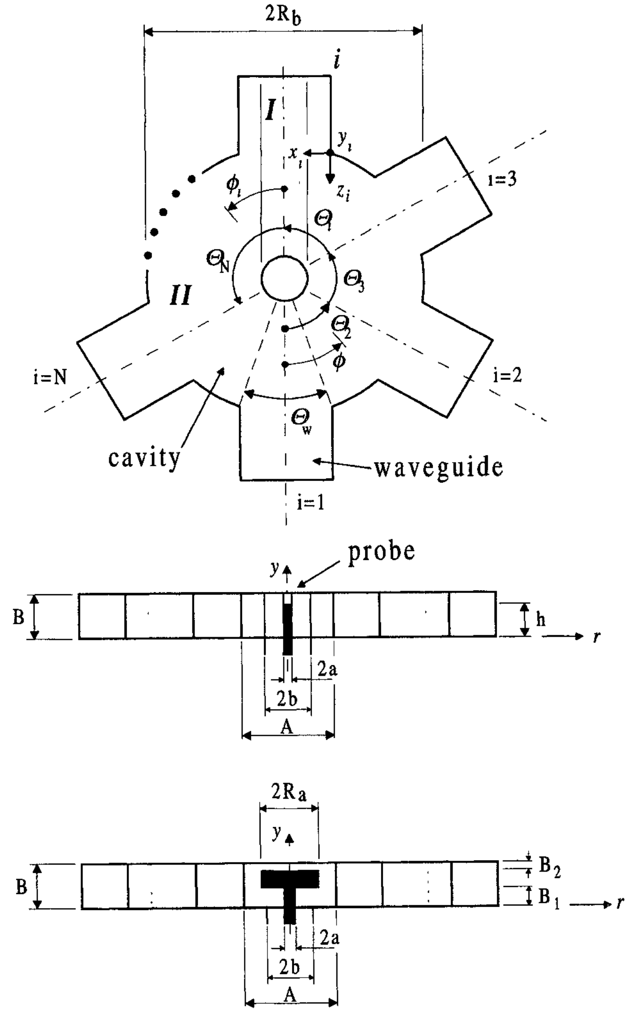

Fig. 1. (Top) Configuration of an N-way divider with a coaxial central probe and H-plane coupled rectangular waveguide ports, (middle) view showing a dielectric coated central probe, and (bottom) view showing a disc-ended central probe.

For a given load impedance Z_{LR} at $r = R_b$, the input impedance Z_{in0} seen at the coaxial port #0 is given by (3)

$$Z_{in0} = Z_{C11} - \frac{Z_{C12} Z_{C21}}{Z_{C22} + Z_{LR}} \tag{3}$$

where Z_{C11}, $Z_{C12}Z_{C21}$, and Z_{C22} are three impedance transformation parameters which at present are unknown.

The impedance transformation parameters can be determined using software [9], [11] which calculates the input impedance at the coaxial port #0 under different load conditions in the radial guide. To solve for Z_{C11}, $Z_{C12}Z_{C21}$, and Z_{C22}, three independent equations have to be generated. These equations can be obtained by calculating three input impedances $Z_{in0}(i)$ for three values of load impedance $Z_{LR}(i)$, $\quad i = 1, 2, 3$ at the cylindrical surface $r = R_b$. The three loads can be a short $Z_{LR}(1) = 0$, an open $Z_{LR}(2) = \infty$ and the radial guide's match termination

$$Z_{LR}(3) = -jZ \frac{H_0^{(2)}(kR_b)}{H_1^{(2)}(kR_b)}$$

where Z is an intrinsic impedance for the radial guide region, k is a wave number, $H_0^{(2)}$, $H_1^{(2)}$ are Hankel functions of 0th and first order and $j = \sqrt{-1}$.

The three equations can be solved in an elementary manner.

Having determined the transformation parameters, the effective radial impedance as observed at $r = R_b$ can easily be calculated and is given by (4)

$$Z_{inR} = Z_{C22} - \frac{Z_{C12}Z_{C21}}{Z_{C11} + Z_C} \tag{4}$$

where Z_c is the impedance seen looking into the coaxial line at port #0.

In particular, expression (4) can be used to determine the radial wave impedance Z_{Rc} as observed at $r = R_b$ when the coaxial line is match-terminated ($Z_c = Z_{cref}$).

B. Modeling of the Peripheral Ports

The peripheral ports can be characterized in terms of the scattering parameters $\{S_{ik}\}$. In order to obtain values of these parameters, the definition requires that one of the peripheral ports is excited and the remaining ports (including the central coaxial port) are match-terminated. It can be assumed that port #1 is an excited port. When the waveguide ports are evenly spread on the radial guide's periphery, the solution to this problem completes the procedure for determining the scattering parameters of the divider. However, if the ports are not evenly spread, the analysis for the remaining ports has to be repeated. This is accomplished by renumbering the ports and by repeating the first part of the analysis.

In order to determine the electromagnetic field which is required in calculations of the scattering parameters, a field matching method can be applied. This method requires that the transverse components of the electromagnetic field be continuous across the common boundary between different regions. Assuming that the cavity region $R_a < r < R_b$ and the waveguides are filled with the same homogeneous dielectric material, the cylindrical boundary $r = R_b$ can be chosen as an interface boundary to match the field between regions I) $r > R_b$ and II) $r < R_b$.

As the field inside the divider cavity is radial TM to y, the only field components which have to be matched at the interface $r = R_b$ are the y-component of the electric field and the ϕ-component of the magnetic field. The required components are given as follows.

The y-component of the electric field in the ith waveguide is given in terms of rectangular waveguide modes (5)

$$E_{yWG} = \sin(k_{x1}x_i)\exp(-\Gamma_{10}z_i)\delta_{1i} + \sum_{m=1}^{\infty} W_{mi}\sin(k_{xm}x_i)\exp(-\Gamma_{m0}z_i) \tag{5}$$

where x_i, y, and z_i are local Cartesian coordinates associated with the ith rectangular waveguide as shown in Fig. 1, $k_{xm} = m\pi/A$, k is a free-space wavenumber, Γ_{m0} is the propagation constant given by equation $\Gamma_{m0}^2 = k_{xm}^2 - k^2$, δ_{1i} is the Kronecker's delta which indicates that the excitation is at port #1, and W_{mi} are unknown field expansion coefficients.

Because the magnitude of the incident wave in waveguide #1 in (5) is assumed to be equal to 1, the coefficients W_{1i} represent the scattering matrix parameters of the divider. In particular, $W_{11} = S_{11}$ represents the reflection coefficient at port #1 and W_{1i}, $i \neq 1$, represents the transmission coefficient S_{i1} between port #1 and port #i, $i = 2, \cdots, N$.

As the electromagnetic fields are to be matched across the circular boundary $r = R_b$, it is more convenient when E_{yWG} in (5) is rewritten in the cylindrical system of coordinates r, ϕ, y (6)

$$\begin{aligned}E_{yWG} = {} & \sin\left[k_{x1}\left(r\sin\phi_i + \frac{A}{2}\right)\right] \cdot \exp\left[\Gamma_{10}(r\cos\phi_i - z_o)\right]\delta_{1i} \\ & + \sum_{m=1}^{\infty} W_{mi}\sin\left[k_{xm}\left(r\sin\phi_i + \frac{A}{2}\right)\right] \cdot \exp\left[-\Gamma_{m0}(r\cos\phi_i - z_o)\right]\end{aligned} \tag{6}$$

where for the region around the ith rectangular waveguide

$$\phi_i = \phi - \theta_i, \quad x_i = r\sin\phi_i + \frac{A}{2}, \quad z_i = z_o - r\cos\phi_i$$

and

$$z_o = R_b\cos\left(\frac{\theta_w}{2}\right).$$

Due to the assumption that the electromagnetic field close to the cavity's side wall is uniform with height, the ϕ-component of the magnetic field in the ith rectangular waveguide can be obtained using the following relationship [14] which holds for TM to y radial fields (7)

$$H_\phi = \frac{-j}{Zk}\frac{\partial E_y}{\partial r}. \tag{7}$$

Using this relationship, the ϕ-component of the magnetic field in the ith waveguide is given by (8)

$$\begin{aligned}H_{\phi WG} = \frac{-j}{Zk}\Bigg\{ & \left\{k_{x1}\sin\phi_i\cos\left[k_{x1}\left(r\sin\phi_i + \frac{A}{2}\right)\right] + \Gamma_{10}\cos\phi_i\sin\left[k_{x1}\left(r\sin\phi_i + \frac{A}{2}\right)\right]\right\} \\ & \cdot \exp\left[\Gamma_{10}(r\cos\phi_i - z_o)\right]\cdot\delta_{1i} + \sum_{m=1}^{\infty} \\ & \cdot W_{mi}\left\{k_{xm}\sin\phi_i\cos\left[k_{xm}\left(r\sin\phi_i + \frac{A}{2}\right)\right] - \Gamma_{m0}\cos\phi_i\sin\left[k_{xm}\left(r\sin\phi_i + \frac{A}{2}\right)\right]\right\} \\ & \cdot \exp\left[-\Gamma_{m0}(r\cos\phi_i - z_o)\right]\Bigg\}.\end{aligned} \tag{8}$$

In the radial cavity, the y-component of the electric field can be expressed in terms of radial TM to y modes [14] which have radial dependence on r and azimuthal dependence on ϕ

as given by (9)

$$E_{yC} = \sum_{p=-\infty}^{\infty} F_p \exp(jp\phi)\, C_p(kr) \tag{9}$$

where F_p are expansion coefficients and functions $C_p(kr)$ are defined by the following expression (10)

$$C_p(kr) = \begin{cases} \dfrac{J_0(kr) + GH_0^{(2)}(kr)}{J_0(kR_b) + GH_0^{(2)}(kR_b)} & \text{for } p = 0 \\ \dfrac{J_p(kr)}{J_p(kR_b)} & \text{for } p \neq 0 \end{cases} \tag{10}$$

where J_p are Bessel functions of pth order, and G is a constant whose value depends on the load impedance at the coaxial line input port #0. Note that $\{C_p(kr)\}$ in (10) are normalized to their value at $r = R_b$, so that $C_p(kr = kR_b) = 1$.

To obtain the value of the constant G in (10), first the ϕ-component of the magnetic field in the cavity region has to be derived. This can be obtained by applying formula (7) to the expression for the y-component of the electric field (9), and is given by (11)

$$H_{\phi C} = \frac{-j}{Z} \sum_{p=-\infty}^{\infty} F_p \exp(jp\phi) C_p'(kr) \tag{11}$$

where

$$C_p'(kr) = \frac{\partial C_p(kr)}{\partial (kr)}.$$

The constant G is obtained from the condition that the radial impedance at $r = R_b$ for the case of the match-terminated coaxial line is equal to Z_{Rc}, as given by (4). Using this condition, constant G is given by (12)

$$G = -\frac{ZJ_0(kR_b) + jZ_{Rc}J_0'(kR_b)}{ZH_0^{(2)}(kR_b) + jZ_{Rc}H_0^{(2)'}(kR_b)}. \tag{12}$$

Having derived full expressions for the y-component of the electric field and the ϕ-component of the magnetic field in the waveguide and cavity regions, the next step is to match these components at the common interface $r = R_b$.

The continuity conditions for the tangential components at $r = R_b$ imply (13)

$$E_{yC} = \begin{cases} E_{yWG} & \text{for } \dfrac{-\theta_W}{2} \leq \phi_i \leq \dfrac{\theta_W}{2} \\ 0 & \text{otherwise} \end{cases} \tag{13a}$$

$$H_{\phi C} = H_{\phi WG} \quad \text{for } \frac{-\theta_W}{2} \leq \phi_i \leq \frac{\theta_W}{2}. \tag{13b}$$

The above equations contain two sets of unknown coefficients: $\{F_p\}$ which describe the field in the cavity and $\{W_{mi}\}$ which describe the field in the individual rectangular waveguides $i = 1, \cdots, N$.

Coefficients $\{F_p\}$ can be eliminated and expressed in terms of coefficients $\{W_{mi}\}$ by multiplying both sides of (13a) by $\exp(-jl\phi)$, $l = 0, \pm 1, \pm 2, \cdots$, and by integrating within the limits $0 < \phi < 2\pi$ [13]. The final set of equations for coefficients $\{W_{mi}\}$ can be obtained by multiplying both sides of (13b) by $\sin[s\pi(\phi_i + \theta_W/2)/\theta_W]$, $s = 1, 2, 3, \cdots$, and by integrating within $-\theta_W/2 \leq \phi_i \leq \theta_W/2$ for each waveguide aperture $i = 1, \cdots, N$. Note that the weighting functions $\sin[s\pi(\phi_i + \theta_W/2)/\theta_W]$ resemble in their behavior the functions $\sin(k_{xs}x_i)$ which were used to describe the rectangular waveguide modes. The final set of equations for the unknown coefficients $\{W_{mi}\}$ can be solved using standard algebraic techniques, such as Gauss' elimination method.

For the case of a symmetric divider, this part of the analysis is sufficient to determine the magnitudes of a full set of scattering parameters for the entire structure. That is, due to the unitary properties of the scattering matrix for a lossless network, it can be shown that

$$|S_{10}|^2 = 1 - \sum_{i=1}^{N} |S_{i1}|^2$$

and

$$|S_{00}|^2 = 1 - N\,|S_{10}|^2 \tag{14}$$

where $S_{i1} = W_{1i}$ are the solutions to the algebraic system of equations when port #1 is excited and the remaining ports are match terminated.

III. Results

Based on the theory described above, computer algorithms have been developed in MICROSOFT FORTRAN for an IBM PC to enable the determination of the scattering parameters of an N-way radial waveguide divider with a central port and rectangular waveguide peripheral ports. One version, called MBCOMBO.FOR was developed for the case of a dielectric coated central probe such as described in [9]. An alternative version, called VWCOMBO.FOR was developed for the case of a disc-ended probe such as described in [11].

In all the algorithms, infinite expansions describing the fields in the rectangular waveguides and the radial cavity were truncated to a finite number of terms. To evaluate 0th and first order Bessel and Neumann functions required in calculations, polynomial approximations [13], [15] were used. Higher order Bessel functions required to evaluate terms $C_p(kr)$ in (9) were calculated using the backward recursion formula [15].

The numerical integrals required in the evaluation of the unknown coefficients $\{W_{mi}\}$ were determined by using piecewise approximations of the integrand in the interval $-\theta_W/2 \leq \phi_i \leq \theta_W/2$ and by simple summations. Because of memory limitations in the PC version of Microsoft Fortran used here, the program was restricted to structures having a maximum of 14 peripheral ports. For arbitrarily positioned peripheral ports, up to ± 20 azimuthal harmonics ($p = -20, \cdots, 0, \cdots, 20$) in the cavity, up to 3 waveguide modes ($m = 1, 2, 3$) in each peripheral port, and up to 20 y-harmonics for the central probe were used in the calculations. For symmetrically positioned peripheral ports, the program was slightly modified so azimuthal harmonics in the form of cosinusoidal functions $\cos(p\phi)$ could be used to expand the field in the cavity. In this case, $p = 0, 1, \cdots, 40$ harmonics were used in the calculations, with the remaining modes numbers the same as for asymmetric structures.

Numerical experiments with the developed algorithms have shown that the solution is fast converging with regard to the number of truncated modes in the cavity and waveguides. This is confirmed through the good agreement between the numerical results obtained with the newly developed algorithms, the Hewlett Packard high frequency structure simulator (HFSS) and measurements, as described below.

To investigate the accuracy of the developed software, the algorithms were first tested for dividers with a small number of ports for which the central probe and the peripheral ports were in close proximitty. In order to investigate the validity of the assumption that the interaction with the central port is mainly due to axially symmetric radial waves, the probe was replaced by a conducting post and functions $C_p(kr)$ in expression (10) were modified to the new form (15)

$$C_p(kr) = \frac{J_p(kr)Y_p(kR_a) - G_pY_p(kr)J_p(kR_a)}{J_p(kR_b)Y_p(kR_a) - G_pY_p(kR_b)J_p(kR_a)} \quad \text{for} \quad p = 0, \pm 1, \pm 2, \cdots \tag{15}$$

where $Y_p(kr)$ are Neumann functions of pth order.

From (15) it can easily be deduced that when for a given p, the coefficient G_p is equal to 1, the function $C_p(kr)$ describes the interaction of the pth azimuthal harmonic with a conducting post of radius R_a positioned at the center of the radial cavity. When $G_p = 0$, $C_p(kr)$ describes the situation when the radial guide is empty.

To investigate the assumptions used in the present analysis, that the peripheral ports interact with the central port mainly due to the axially symmetric cavity modes, two cases were considered.

1) When the interaction between the waveguide ports and the central post is described in an exact manner: $G_p = 1$ for all values of p.
2) When the interaction between the waveguide ports and the central post is approximated, so that $G_0 = 1$, and $G_p = 0$ for $p \neq 0$.

Fig. 2 shows a comparison between the results for the scattering parameters of a symmetric 4-port with a conducting central post obtained with program MBCOMBO.FOR for the two investigated cases. It can be noticed that for a relatively thin conducting post (diameter $2R_a = 4.10$ mm $= 0.14$ $\lambda_{10\,\mathrm{GHz}}$), the results for S_{11} and S_{31} calculated using the two alternative approaches (exact and approximate) differed only by 0.3 dB in the worst case across the full waveguide band. Parameter S_{21} seemed to be unaffected by the way it was calculated. Similar calculations for a relatively thick conducting post (diameter $2R_a = 7$ mm $= 0.233$ $\lambda_{10\,\mathrm{GHz}}$) have shown that the results for S_{11} and S_{31} calculated using the two alternative approaches differed by 0.7 dB in the worst case across the full waveguide band. As before, parameter S_{21} seemed to be unaffected by the way it was calculated. These results support the assumption that for the N-way divider, the interaction between the peripheral ports and the central probe is mainly due to the axially symmetric radial waves.

Next, a symmetrical divider with a dielectric coated coaxial probe partially spanning the cavity height was considered. Fig. 3 shows a comparison between the results for the scattering parameters of an X-band, symmetric 4-way divider obtained with the newly developed field matching method

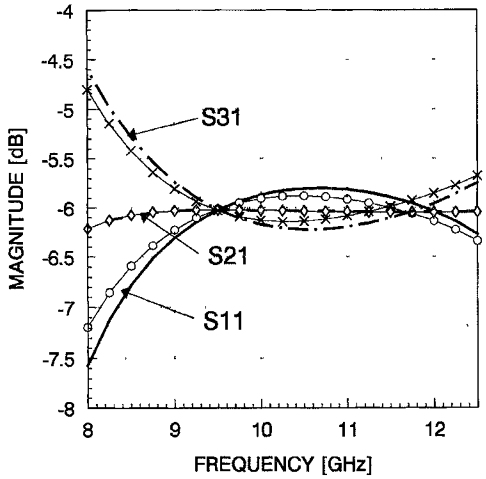

Fig. 2. Comparison between computational results for the scattering parameters of a symmetrical X-band 4-port with a conducting central post. Device dimensions [mm]: radial cavity $R_a = 2.05$, $R_b = 21.50$; waveguide: $A = 22.86$, $B = 10.16$; post: radius $= R_a$, height $= B$. $G_0 = 1$, $G_p = 0$ for $p \neq 0$: ——, - - -, —·—·—; $G_p = 1$ for all p: —o—, ——◇——, ——×——.

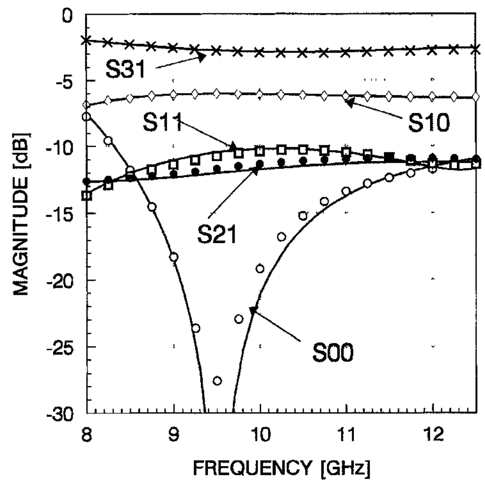

Fig. 3. Comparison between computational results for the scattering parameters of a symmetrical X-band 4-way divider with a dielectric coated central probe. Device dimensions [mm]: radial cavity $R_a = 3.45$, $R_b = 21.50$; waveguide: $A = 22.86$, $B = 10.16$; Probe: $a = 1.0$, $b = R_a$, $h = 5.10$; dielectric surrounding probe: $\varepsilon_1 = \varepsilon_2 = 2.1\varepsilon_0$. FMM (MBCOMBO): ——; FEM (HFSS): o, ◇, □, •, ×.

(FMM) algorithm MBCOMBO.FOR and the commercial finite element method (FEM) software high frequency structure simulator (HFSS), by Hewlett Packard. Note that in this example, the probe (diameter $2a = 2$ mm $= 0.066$ $\lambda_{10\,\mathrm{GHz}}$) was relatively thin. However, it had a relatively thick dielectric coat (diameter $2R_a = 6.9$ mm $= 0.23$ $\lambda_{10\,\mathrm{GHz}}$).

Good agreement between the two software packages for all the scattering parameters can be observed across the full waveguide band. The slight discrepancies between them may be due to the approximations made in the present theory. Although good agreement is observed between FMM and FEM, there are significant differences in the computational time and the memory requirements for two software packages. The analysis of the 4-way divider using the FMM required less than 60 kB of memory. The computational time for ±20

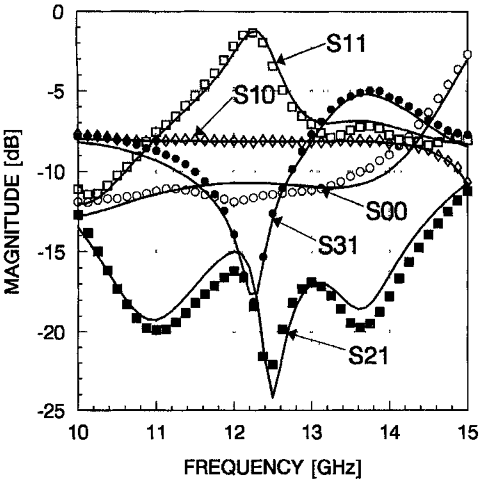

Fig. 4. Comparison between computational results and measurements for selected scattering parameters of a symmetrical Ku-band 6-way divider with a disc-ended central probe. Device dimensions [mm]: radial cavity $R_a = 2.05$, $R_b = 30.40$; waveguide: $A = 19.05$, $B = 9.525$; Probe: $a = 0.635$, $b = 2.05$, disc radius $= R_a$, $B_1 = 2.0$, $B_2 = 2.1$; dielectric: air throughout. FMM (VWCOMBO): ——; Measured: o, ◇, □, ■, •.

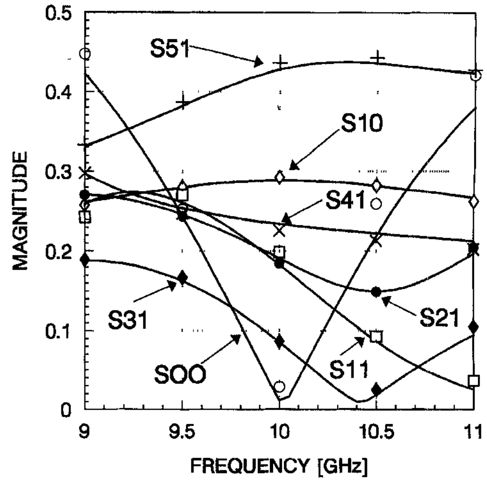

Fig. 5. Comparison between computational results for selected scattering parameters of a symmetrical X-band 12-way divider with a dielectric coated central probe. Device dimensions [mm]: radial cavity $R_a = 2.05$, $R_b = 41.90$, waveguide: $A = 19.05$, $B = 9.525$; Probe: $a = 0.635$, $b = 2.05$, $h = 6.80$; dielectric surrounding probe: $\varepsilon_1 = \varepsilon_2 = 2.1\varepsilon_0$. FMM (MBCOMBO): ——; FEM (HFSS): o, ◇, □, •, ♦, ×, +.

azimuthal modes and $M = 3$ rectangular waveguide modes in each waveguide port at a single frequency point was less than 2 s for a 33 MHz 486 PC. The FEM based HFSS required 64 MB of RAM with temporary files of 30 MB in size being generated during the solution process. Each point in the frequency sweep took close to 30 min, using a mesh adaptively optimized at the highest investigated frequency to meet the convergence criterion of $\Delta S = 0.02$.

In order to obtain further confidence in the validity of the developed software, it was tested against experiment. Fig. 4 shows a comparison between the results for selected scattering parameters of a Ku-band, symmetric 6-way divider obtained with the newly developed algorithm VWCOMBO.FOR and measurements. The experimental results were obtained using a Hewlett Packard 8510C vector network analyzer. Good agreement between the FMM software and measurements is observed. The slight discrepancies may be due to the approximate nature of the FMM analysis as well as due to dimensional or measurement errors.

To further demonstrate the versatility of the developed software, a more practical divider with 12 output ports was also analyzed. Fig. 5 shows a comparison between FMM and FEM for selected scattering parameters of the analyzed device. Again, good agreement between the two software (FMM and FEM–HFSS) packages is observed. The slight discrepancies are again probably due to the approximations made in the FMM analysis. The divider features high return loss of the central probe and moderate isolation (on average) between the peripheral probes across the 9.8 and 10.2 GHz frequency band. In comparison with the dividers equipped in coaxial peripheral probes, such as considered in [7], [8], the currently investigated divider with the rectangular waveguide output ports seems to have a narrower operational bandwidth as far as the return loss of the central probe is concerned. This could be due to a different mechanism in terms of how the central probe matching is accomplished. In dividers with probe-type ports,

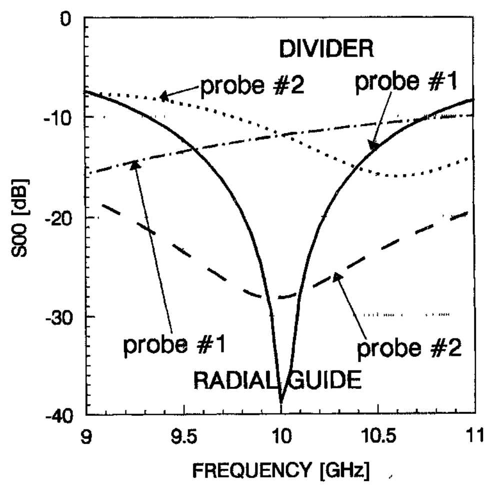

Fig. 6. Comparison between the return loss of a dielectric coated probe in an infinite radial guide and as the central probe of a 12-way radial divider. Probe #1: $h = 6.80$ mm; probe #2: $h = 5.75$ mm. The remaining dimensions of the radial divider and probe are the same as for Fig. 5.

well designed peripheral probes provide a good approximation to an absorbing boundary for a radial wave launched from the central port. In the present divider, waveguide peripheral ports seem to provide only a rough approximation to the absorbing wall case. To demonstrate this situation clearly, the following computational experiments were performed. Fig. 6 shows the return loss as observed by a dielectric coated probe of two different heights, $h = 6.8$ mm (probe #1) and $h = 5.75$ mm (probe #2). It can be seen that when probe #1 is located in the 12-way divider, it produces a 20 dB return loss in a narrow band centered at 10 GHz. The same probe produces return loss between 10–15 dB in the 9–11 GHz frequency band in an infinite radial guide. Probe #2 produces a return loss greater than 18 dB across the 9–11 GHz band in an infinite radial guide but only 8–15 dB return loss in the 12-way radial divider.

For the divider, a good impedance match of central probe #1 seems to be obtained via the interaction between the waveguide ports, the exposed conducting parts of the side wall and the central probe. This match becomes rather narrowband in nature. Simulations with probe #2 indicate that a wider impedance bandwidth could be obtained if the peripheral ports emulated an absorbing wall. This was the case for the divider with peripheral coaxial probes described in [7].

Therefore, to obtain a larger bandwidth for the impedance match of the central probe in the divider with the waveguide output ports, additional matching elements need to be introduced to make peripheral ports behave more effectively as an absorbing boundary. For example, inductive or capacitive diaphragms in the waveguide peripheral ports and resistive vanes at the cavity's side walls may be used for this purpose. This problem, however, is left for future studies.

IV. Conclusion

A field matching technique for the analysis of an N-way radial waveguide divider with a coaxial central port and rectangular waveguide peripheral ports has been presented. Dielectric coated and disc ended probes have been considered at the central port. The analysis has been divided into two parts, namely the modeling of the central probe and the modeling of the waveguide peripheral ports. It has been shown that the analysis can be considerably simplified by assuming that the peripheral ports interact with the central port by means of axially symmetric radial waves which are uniform with cavity's height. Azimuthally and height varying radial waves produced by the peripheral ports or the central probe have been neglected while considering this interaction. Based on this analysis, computer algorithms for determining the scattering parameters of the device have been developed. These algorithms have been tested on the examples of 4, 6, and 12-way dividers, and have been compared against a more involved commercial finite element package (HFSS) and against experiment. Good agreement between these results has been noted, proving that the developed computer algorithms may be confidently used for the analysis and design of radial waveguide dividers with waveguide output ports.

References

[1] K. J. Russel, "Microwave power combining techniques," *IEEE Trans. Microwave Theory Tech.*, vol. MTT-27, pp. 472–478, May 1979.

[2] K. Chang and C. Sun, "Millimeter-wave power-combining techniques," *IEEE Trans. Microwave Theory Tech.*, vol. 31, pp. 91–107, Feb. 1983.

[3] B. J. Sanders, "Radial combiner runs circles around hybrids," *Microwave*, pp. 55–58, Nov. 1980.

[4] S. J. Foti, R. P. Flam, and W. J. Scharpf, Jr., "60-way radial combiner uses no isolators," *Microwaves and RF*, pp. 96–118, July 1984.

[5] M. E. Bialkowski, "Modeling of the coaxial-waveguide power-combining structure," *IEEE Trans. Microwave Theory Tech.*, vol. MTT-34, no. 9, pp. 937–942, 1986.

[6] K. Fukui and S. Nogi, "Mode analytical study of cylindrical cavity power combiners," *IEEE Trans. Microwave Theory Tech.*, vol. MTT-34, no. 9, pp. 943–951, 1986.

[7] M. E. Bialkowski and V. P. Waris, "Electromagnetic model of a planar radial-waveguide divider/combiner incorporating probes," *IEEE Trans. Microwave Theory Tech.*, vol. 41, nos. 6/7, pp. 1126–1134, June/July 1993.

[8] S. Nogi, M. Kojima, and K. Fukui, "A broadband conical-radial wave power divider/combiner," in *Proc. 1994 Asia-Pacific Microwave Conf.*, Tokyo, pp. 507–510.

[9] M. E. Bialkowski, "Analysis of a coaxial-to-waveguide adaptor incorporating a dielectric coated probe," *IEEE Microwave & Guide Wave Lett.*, vol. 1, no. 8, pp. 211–214, 1991.

[10] R. B. Keam and A. G. Williamson, "Analysis and design of coaxial-line/rectangular waveguide junction with a dielectrically sheathed center probe," in *Proc. 1992, Asia-Pacific Microwave Conf.*, Adelaide, pp. 845–848.

[11] M. E. Bialkowski, "Analysis of a coaxial-to-waveguide adaptor including a disc ended probe and a tuning post," *IEEE Trans. Microwave Theory Tech.*, vol. MTT-43, no. 2, pp. 344–349, Feb. 1995.

[12] P. W. Davis and M. E. Bialkowski, "Performance of field matching and finite element methods on practical coaxial-to-waveguide transitions," *J. Elec. Electron. Eng.*, vol. 15, no. 1, pp. 23–29, Mar. 1995.

[13] M. E. Bialkowski, "Analysis of an N-port consisting of a radial cavity and E-plane coupled rectangular waveguides," *IEEE Trans. Microwave Theory Tech.*, vol. 40, no. 9, pp. 1840–1843, Sept. 1992.

[14] R. F. Harrington, *Time Harmonic Electromagnetic Fields.* New York: McGraw-Hill, 1961, ch. 5.

[15] M. Abramovitz and I. A. Stegun, *Handbook of Mathematical Functions.* Dover Publications, 1965.

Marek E. Bialkowski (SM'88) received the M.E.S. degree (1974) in applied mathematics and the Ph.D. degree (1979) in electrical engineering, both from the Warsaw Technical University, Warsaw, Poland.

In 1977, he joined the Institute of Radioelectronics, Warsaw Technical University, and in 1979 became an Assistant Professor. In 1981, he was awarded a Postdoctoral Research Fellowship by the Irish Department of Education and spent one year at the University College Dublin carrying out research in the area of microwave circuits. In 1982, he won a Postdoctoral Research Fellowship from the University of Queensland, Brisbane, Australia. During his stay in Brisbane he worked on the modeling of millimeter-wave guiding structures (particularly on waveguide diode mounts). In 1984, he joined the Department of Electrical and Electronic Engineering, James Cook University, Townsville, Australia, as a Lecturer in the field of communications. In 1986 he was promoted to Senior Lecturer. In 1988, he was a Visiting Lecturer in the Department of Electronics and Computer Science, University of Southampton, U.K. He was invited to lecture in the field of antenna theory and design. Since 1989, he has been with the Department of Electrical Engineering at the University of Queensland, Brisbane, Australia where he is the Head of the Microwave and Antenna Group. In 1994, he held an appointment as a Visiting Professor in the Department of Electrical and Computer Engineering in the University of Victoria, Victoria, Canada.

Dr. Bialkowski is a member of the Editorial Board for the IEEE Transactions on Microwave Theory and Techniques. Also, he is a member of the Editorial Board for the Asia-Pacific Engineering Journal. His interests include computational electromagnetics, antennas for mobile satellite communications, low profile antennas for reception of satellite broadcast TV programs, near-field/far-field antenna measurements, quasioptical power combining techniques, six-port techniques, and industrial applications of microwaves. He has published extensively in all these areas. His name is listed in a number of international biographical references: *Marquis Who's Who in the World*, *Who's Who in Science and Engineering*, *Dictionary of International Biography* (Cambridge, U.K.) and the *World Book of Bialkowskis*.

Vesa P. Waris (S'91) was born in Pello, Finland, in 1967. He received the B.E. degree from the University of Queensland, Brisbane, Australia, in 1988. He is currently completing his Ph.D. degree at the University of Queensland.

Since 1989, he has worked for MITEC Ltd. as a Design Engineer, with projects including the L-band Radioastron receiver, phase-locked oscillators, a 30-GHz receiver using packaged HEMT's, and various satellite earth-station equipment. He is currently researching power combiners and dividers.

Mr. Waris holds an Australian Postgraduate Award.